Characterization of sudden and sustained base flow jump hydrologic behavior in the humid seasonal tropics of the Panama Canal Watershed

Running head: Sudden and sustained increase in tropical base flow

Yanyan Cheng [1, 3 *], Fred L. Ogden [2], Jianting Zhu [3]

[1] Currently at Atmospheric Sciences and Global Change Division, Pacific Northwest National Laboratory, Richland, WA, 99354, USA

[2] Currently at University Corporation for Atmospheric Research, Cooperative Programs for Earth System Sciences, NOAA/NWS/Office of Water Prediction, U.S. National Water Center, Tuscaloosa, AL 35401, U.S.A., Formerly at University of Wyoming.

[3] Department of Civil and Architectural Engineering, University of Wyoming, Laramie, WY 82071, U.S.A.

* Corresponding author: Yanyan Cheng (yanyan.cheng@pnnl.gov)

Keywords: Wet season; Tropical catchment; Base flow; Sustained base flow increase; Sensitivity analysis; Correlated parameters; Panama, land cover effect

Acknowledgments

The authors would like to express our great appreciation to the Panama Canal Authority for providing all the hydrological data used in this study. The Meteorological and Hydrological Branch, Panama Canal Authority, Republic of Panama (http://www.pancanal.com) was acknowledged. The 10m canopy height corrected DEM was provided by Dr. Robert F. Stallard of Smithsonian Tropical Research Institute. This work was funded by the U.S. National Science Foundation (NSF) EAR-1360384 WSC-Category 2 Collaborative Research: Planning and Land Management in a Tropical Ecosystem: Complexities of Land-use and Hydrology Coupling in the Panama Canal Watershed, and the Smithsonian Tropical Research Institute. Graduate student support while the first author was at the University of Wyoming was partially provided by the Wyoming Center for Environmental Hydrology and Geophysics (WyCEHG) funded by NSF EPS-1208909.

ABSTRACT:

Base flows are important for tropical regions with pronounced dry seasons which are facing increasing water demands. Base flow generation, however, is one of the most challenging hydrological processes to characterize in the tropics. In many years during the May-December wet season in the Panama Canal Watershed (PCW), base flows in rivers abruptly increase. This increase persists until the start of the December-April dry season. Understanding this unusual base flow jump (BFJ) behavior is critical to improve water provisioning in seasonal tropics, especially during droughts and extended dry seasons. This study developed an integrated approach combining piecewise regression on cumulative average base flow and sensitivity analysis to calculate the timing and magnitude of BFJ. Rainfall, forest cover, mean land surface slope, catchment area and estimated subsurface storage were tested as predictors for the occurrence and magnitude of the BFJs in seven sub-catchments of the PCW. Sensitivity analysis on correlated predictors allowed ranking of predictor contributions due to isolated and cross correlation effects. Correlations between observed BFJs and BFJs predicted by watershed and rainfall-related predictors were 0.92 and 0.65 for BFJ timing and magnitude, respectively. Forest cover was the second most significant predictor after cumulative rainfall for jump magnitude, owing to larger subsurface storage and groundwater recharge in forests than pastures. Catchments in the mountainous eastern PCW always generated larger jumps due to their higher rainfall and greater forest cover than the western PCW catchments. The cross-correlations between predictors contributed to more than 50% of the jump variances. The results demonstrate the importance of rainfall gradient and catchment characteristics in affecting the sudden and sustained BFJs, which can help inform land management decisions intended to enhance water supplies in tropics. This study underscores the need for more research to further understand the

hydrological processes involved in the BFJ phenomenon, including better BFJ models and field characterizations, to help improve tropical ecosystem services under a changing environment.

1. Introduction

Knowledge of quantities and temporal patterns of base flow aids in understanding of hydro-environmental sustainability, water quality and quantity management, agriculture, and more generally the food-energy-water nexus, especially in tropical catchments with remarkable dry and wet seasons which are facing increasing water demands under global changes (Price 2011; Bruijnzeel, 2004; Wohl et al., 2012; Ogden et al., 2013, Cook et al., 2014). Better understanding of base flow characteristics may help guide land management decisions with the aim of enhancing water resources provisioning and hydro-ecosystem services in tropics. However, limited knowledge is available about base flow generation in tropical catchments (Muñoz-Villers et al., 2016).

Pena-Arancibia et al. (2010) analyzed the potential of climatic and terrain attributes (e.g., catchment shape, morphology, land cover, soils and geology) of tropical catchments in predicting base flow recession rates and concluded tree cover and catchment slope were good predictors. Muñoz-Villers et al. (2016) found that the main factors controlling stream water mean transit time included land cover, catchment slope, and the permeability at the soil–bedrock interface. Cadol et al. (2012) studied the effect of evapotranspiration (ET) on base flow in a low-gradient tropical headwater catchment in Costa Rica and found that forest exerted influence on streamflow in recession periods through changes in ET. Krishnaswamy et al. (2013) examined the groundwater recharge response and hydrologic services on evergreen tropical forest and degraded tropical forest ecosystems in western India. Their results supported the "infiltration-

evapotranspiration trade-off" hypothesis that the differences in infiltration between land covers controlled the differences in groundwater recharge and dry-season flow. Zhang et al. (2019) explored the ecological and hydrological functioning of a "reforested" tropical catchment and found that forest development over two decades caused streamflow to become perennial. These results highlighted the importance of climatic as well as terrain factors, such as catchment slope and land covers, in controlling groundwater recharge and base flows.

Panama lies in one of the seasonal tropics (Callaghan and Bonell, 2005; Montgomery Watson Harza, 2001) and plays an important economic role as shipping through the Panama Canal represents approximately 3% of global maritime commerce and 19% of trade between the U.S. and Asia. Ships using the Panama Canal are lifted by locks to transit the isthmus of Panama via Lake Gatun. Fresh water is needed every time a ship is raised to or lowered from Lake Gatun. That fresh water to sustain the Canal operation is supplied by runoff from the Panama Canal Watershed (PCW). The Canal expansion project completed in 2016 further increased water demand for the PCW (Knight 2008). Groundwater-fed base flows in the PCW are therefore important to sustain Canal operations, particularly during droughts such as those related to El Nino (Bretfeld et al., 2018) and during the extended dry seasons (Cheng et al., 2018). In addition, the Panama Canal Authority is willing to offer contracts to private farmers to change land use to increase provisioning of ecosystem benefits including dry-season water flows (Adamowicz et al., 2019). This creates a need to better understand the quantities and temporal patterns of base flow behaviors under different land covers in the PCW, to examine the water availability to sustain the Canal operation (Knight 2008) and rapid population growth (Bonell & Bruijnzeel, 2005).

In most years during the latter half of the wet season, the base flow in sub-catchments of the PCW increases to a new level and remains at this new elevated level for the remainder of the wet

season (Niedzialek, 2007). Niedzielek & Ogden (2005) and Niedzialek (2007) reported and discussed this step-wise increase behavior in base flows, but its statistical characteristics and triggering factors including the effects of land cover and rainfall characteristics remained to be resolved. While knowledge of general behavior of base flow is important to the issue of water quantity and quality, we also need to investigate this unique but poorly understood BFJ phenomena to understand unusual patterns of low flows in the seasonal tropics. This knowledge affects water resources availability and more broadly hydrological ecosystem services during times of drought and pronounced dry season (Ogden et al., 2013).

Many studies have sought to establish correlations between climate and topographic predictors and base flow statistics. van Dijk (2010) evaluated daily streamflow data in 183 Australian catchments and reported that rainfall and climate indices predict 70-84% of the variations in low- and quick-flows. By using streamflow observations from 3394 catchments, Beck et al. (2013) examined global patterns of base flow index and base flow recession constant based on 18 climatic and physiographic characteristics. One main deficiency of many previous studies relating climate and topographic predictors to base flow statistics is that they did not fully consider the cross-correlation between these predictors, which is frequently observed and has important effect on estimating base flow statistics. In order to understand sources of uncertainty in the base flow statistics and attribute it to predictors, it is critical that the cross-correlation among predictors be addressed in the context of base flow behavior predictions.

The objective of this study was to better understand the hydrological processes and contributing factors underlying the observed sudden and sustained increases in base flows with the ultimate goal of improved quantitative characterization and predictive ability of BFJs. To support these objectives, we developed an integrated approach to objectively detect and

quantitatively define BFJ timing and magnitude based on a piecewise linear regression on cumulative average base flow. The analysis was performed using daily streamflow, rainfall data and watershed characteristics from seven sub-catchments in the PCW. Two base flow separation techniques were selected to investigate the sensitivity of jump detection to base flow separation methods. BFJs occurring in the eastern and western PCW catchments were separated to investigate the effect of climatology and watershed attributes. Specifically, we examined three watershed and four rainfall-related predictors to explain the variance in both timing and magnitude of BFJs. After identifying the main predictors to the BFJ behavior, we performed a sensitivity analysis to rank the relative importance of the predictors and quantify their independent (or uncorrelated) contributions and contributions caused by the cross-correlations between these predictors.

To the best of our knowledge, the timing and magnitude of the BFJ behavior have not previously been quantified in relation to the cross-correlated factors that trigger this BFJ behavior, particularly in the tropics where large populations are often dependent upon water supply from small and data-poor watersheds that are highly susceptible to drought. Improving delivery of base flow may be possible through land management decisions supported by the improved understanding sought in this study.

2. Study area and Data

The 3300 km^2 Panama Canal Watershed (PCW) is located on the Isthmus of Panama, between the Caribbean Sea and Pacific Ocean (Figure 1). The PCW is underlain by deeply weathered basaltic and andesitic parent rocks (Harmon, 2005a, 2005b; Stewart et al., 1980; Wörner et al., 2005), with Oxisols soils formed from *in situ* weathering of bedrock (Turner and

147 Engelbrecht, 2010), which is up to 20 m in depth (Ogden et al., 2010). Panama has pronounced
148 dry and wet seasons (Ogden et al., 2013; Cheng et al., 2017) due to motion of the Inter-Tropical
149 Convergence Zone (ITCZ). While the ITCZ is north of Panama from late April or early May to
150 December, frequent cloud cover and rainfall dominate the wet season. When the ITCZ is south
151 of Panama during December or early January to April, Panama undergoes a dry season and
152 experiences warmer and drier climate with very little rainfall. In this study, we chose 1 May to
153 31 December as the wet season period to examine the BFJ phenomena.

154 **Figure 1**

155 The Panama Canal from the Caribbean Sea to the Pacific Ocean runs mainly north-south, and
156 approximately divides the PCW into eastern and western halves. The mountains in the eastern
157 PCW are considerably taller and more numerous than those in the western half. Owing to
158 differences in orography, the annual rainfall in catchments in the eastern PCW exceeds that in
159 the western PCW by about 1000 mm y^{-1}. As a result, catchments in the eastern PCW produce
160 considerably more runoff (Harmon et al. 2009) compared to the western half of the PCW. The
161 fraction of catchments under forest land cover is also higher in the eastern PCW. It is therefore
162 important to distinguish the BFJ characteristics for catchments located at eastern and western
163 PCW.

164 Many tropical watersheds suffer from data scarcity and quality issues with scant streamflow
165 records (Zhang 2018). This study used rainfall and runoff data provided by the Panama Canal
166 Authority of seven sub-catchments throughout the western and eastern PCW with most complete
167 and recent records. These seven catchments are the principal suppliers of water in the PCW and
168 represent the climate and topographic ranges of the PCW.

169 Land covers of the seven study catchments in 2008 are shown in Figure 1. Data availability

and physiographic characteristics in the seven study catchments are summarized in Table 1. Land cover variation is an important feature of these catchment data sets and the mature forest fractions listed in Table 1 vary from 0.1% to 96%. Catchment mean elevation and mean land surface slope were derived using a canopy height corrected, 10-meter resolution digital elevation model. The drainage area of the study catchments ranges from 67 to 407 km^2, the mean elevation ranges from 110 m to 460 m above mean sea level, and the mean land surface slope varies from 7 to 20 degrees. Rainfall and streamflow data originally at 15-minute interval were converted to daily time series. Streamflow data were normalized by the drainage areas to facilitate comparison among different catchments of different sizes. The rainfall depth for each catchment was calculated by taking the average of rainfall from all available rainfall gauges within the catchment (Table 1). The lengths of data record for both rainfall and streamflow series at each catchment are listed in Table 1.

Table 1

3. Methods

An automatic method to detect BFJ timing and magnitude aided in evaluating the causes of BFJs. This algorithm consists of four primary steps. Each step is described from Section 3.1 to 3.3 below and schematically shown in Figure 2 using observed data during the wet season at the Gatun catchment in PCW as an example. Section 3.4 describes how we choose the contributing predictors for BFJ. Section 3.5 describes the approach to apportion the relative contributions to the BFJ variances from various contributing predictors.

In Step 1, we separated base flow from the original daily streamflow data year by year (Figure 2a). In Step 2, we calculated cumulative average base flow during the wet season. Since a sharp increase or decrease shifts the cumulative average base flow series upward or downward,

193 we can quantify the BFJ timing based on where the slope of the cumulative average base flow
194 time series changes from almost zero to a positive value (Figure 2b). In Step 3, we applied a
195 piecewise linear regression on the cumulative average base flow to fit two separate lines with
196 distinct slopes. The change point between these two fitted lines is when a BFJ occurs (Figure 2b).
197 In Step 4, we calculated BFJ magnitude as the difference between average base flow before and
198 after the jump timing.

199 We separated BFJs at two locations to account for the differences (e.g., annual rainfall, slope,
200 forest cover) of catchments located at western and eastern PCW. We identified three watershed
201 predictors and four rainfall-related predictors to explain BFJ and performed sensitivity analysis
202 to rank the relative importance of these predictors.

203 There are several methods on change point detection (e.g., Ivancic and Shaw, 2017; Xiong et
204 al., 2015). Ivancic and Shaw (2017) detected multiple change points in annual streamflow using
205 all the U.S. Geological Survey flow gages and attributed the cause of the abrupt changes in
206 streamflow to natural variability in the climate signal. Xiong et al. (2015) proposed a three-step
207 framework to detect change point for multivariate flood series by distinguishing the change
208 points in both marginal distributions and dependence structure. Our study focused on base flow,
209 which is important to sustain water provisioning in the seasonal tropics, especially during the dry
210 periods and under drought conditions. In addition, we quantified both BFJ timing and magnitude
211 and conducted a sensitivity analysis to attribute the abrupt changes in base flows to both
212 precipitation and watershed characteristics (e.g., land cover, catchment slope), which has been
213 identified as crucial factors influencing base flow in tropical montane watersheds (Muñoz-Villers
214 et al., 2016).

215 **3.1 Base flow separation**

Many base flow separation methods have been proposed, including chemical tracers and isotopic methods (Ladouche et al., 2001), graphical methods (Chow et al., 1988) and filtering methods (Lyne & Hollick, 1979; Nathan & McMahon, 1990; Chapman, 1991; Chapman & Maxwell, 1996; Arnold & Allen, 1999; Eckhardt, 2005; Aksoy et al., 2009). Since geochemical or isotopic data were not generally available, two easily automated, objected, and reproducible digital filtering methods were used to separate base flows in this study to examine the subjectivity and sensitivity of base flow separation methods in BFJ detection.

The first method was the digital filter developed by Eckhardt (2005) (hereafter referred to as E2005). The first parameter of Eckhardt's filter is the base flow recession parameter *a*. By assuming that the outflow from the aquifer is linearly proportional to its storage, the recession parameter *a* is calculated as the slope of the straight line when we plot log *Q* against time. The second parameter is the maximum value of the base flow index (BFI_{max}), which is determined based on the backward filtering operation approach proposed in Collischonn & Fan (2013) (Equations 1 to 3).

$$\mathrm{BFI}_{\max} = \frac{\sum_{i=1}^{N} BMAX_i}{\sum_{i=1}^{N} Q_i} \tag{1}$$

where *i* is the current time step, *N* is the total numbers of data points, *Q* is streamflow (L T^{-1}), and *BMAX* is the maximum base flow calculated using Equation 2 (L T^{-1}):

$$BMAX_j = \frac{Q_{j+1}}{a}, \quad j = N-1, \ldots 1 \tag{2}$$

subject to $BMAX_j < Q_{j+1}$.

After obtaining the values of *a* and BFI_{max}, base flow *B* (L T^{-1}) is calculated using the following equation:

$$B_i = \frac{(1 - \mathrm{BFI_{max}}) \times a \times B_{i-1} + (1 - a) \times \mathrm{BFI_{max}} \times Q_i}{1 - a \times \mathrm{BFI_{max}}} \quad (3)$$

subject to $B_i \leq Q_i$.

However, base flow separated using this method may contain high discharge peaks in response to antecedent rainfall events. Such temporary increases in base flow should not sustain after the rainfall events and should not be characterized as BFJs. To complement this, we adopted the method proposed by Brutsaert (2008) (hereafter referred to as B2008) to maximize the likelihood of selecting sustained BFJs during recessions. Technically, we selected the last streamflow values when direct runoff ends between the antecedent and coming rainfall events, which is the lowest point of streamflow during each recession and can generally remove the effect of antecedent rainfall events.

3.2 Cumulative average base flow

We then calculated the cumulative average base flow during the wet season (Figure 2b) using Equation 4, which considers the effect of the current data point on the time series prior to this point.

$$B_{cai} = \frac{\sum_{k=1}^{i} B_k}{i} \quad (4)$$

where k is the daily date index, i is the averaging time span (T), B_k is the base flow on the k-th day (L T^{-1}), and B_{cai} is the cumulative average base flow on the i-th day (L T^{-1}).

We proposed this efficient method by using the time series of cumulative average base flow rather than the simple cumulative base flow. In the simple cumulative base flow plot, a BFJ would only manifest as two segments with different slopes. However, the same sustained BFJ is reflected as a slope increase from almost zero to a distinct positive slope in the time series of cumulative average base flow, evident from the series after the change date in Figures 2b.

Therefore, using the time series of cumulative average base flow is easier to quantitatively detect the BFJs that may exist.

3.3 Calculation of BFJ timing and magnitude

After producing the cumulative average base flow time series over the wet season, a python code of piecewise linear regression (https://github.com/DataDog/piecewise) was used to automatically detect the point in time when the base flow jump occurs, by minimizing the errors of ordinary least squares regressions for the two segments of cumulative average base flow time series before and after the jump. The piecewise linear regression fits two separated lines with distinct slopes for the cumulative average base flow series as shown in Figures 2b. The change point is when the jump occurs. The change magnitude was then calculated by the difference between the mean values of the base flow periods before and after the change date as given in Equation 5:

$$\Delta y = \frac{\sum_{i=N_1+1}^{N_1+N_2} B_i}{N_2} - \frac{\sum_{i=1}^{N_1} B_i}{N_1} \quad (5)$$

where Δy is the BFJ magnitude (L T^{-1}) and N_1 and N_2 are the numbers of data points before and after the change point, respectively.

3.4 Predictors tested to explain BFJ timing and magnitude

Base flow is a slow process, resulting from discharge of groundwater to streams (van Dijk, 2010). BFJs should obviously depend on rainfall, as the abrupt and sustained increases in base flow seem to follow a rainfall event (Niedzialek, 2007). In addition, both van Dijk (2010) and Pena-Arancibia et al. (2010) reported the effects of watershed attributes such as catchment shape and land cover on base flow recession, which explains 20% of variation in average base flow and quick flow. Based on these findings, we tested four rainfall-related predictors and three

watershed characteristics in terms of their ability to predict the observed BFJ behavior. The three watershed attributes considered include: fraction of mature forest land cover (f_{for}), catchment area, and catchment mean land surface slope. The four rainfall related factors are: (1) cumulative rainfall depth from the start of the wet season to the occurrence of the BFJ (P_{cum}), (2) subsurface storage changes (S_{gw}) before the jump occurrence, estimated as cumulative rainfall minus cumulative runoff minus cumulative ET as explained below, (3) cumulative rainfall of three rainfall events before the jump occurrence (P_e), and (4) maximum rainfall intensity of three rainfall events before the jump timing (I_e). While the cumulative rainfall and subsurface storage changes are conceivable factors responsible for base flow jumps, we also included rainfall characteristics of three rainfall events prior to the jumps that may also directly trigger base flow jumps. We included only up to three events (i.e., one, two, or three) prior to the base flow jump to investigate whether the jump may be triggered due to instantaneous response to only a few recent events.

Since direct observations of subsurface storage were not available, we applied a water balance method to estimate the BFJ predictor related to changes in subsurface storage S_{gw}:

$$S_{gwi} = \sum_{k=1}^{i} P_k - \sum_{k=1}^{i} ET_k - \sum_{k=1}^{i} R_k \quad (6)$$

where i is the number of days considered prior to the sustained BFJ, S_{gwi} is the subsurface storage changes on the i-th day (L), P_k is rainfall (L), ET_k is estimated evapotranspiration (L), R_k is runoff depth (L) on the k-th day.

Owing to seasonality, ET in the PCW exhibits considerable intra-annual variability. ET also varies considerably between different land covers, with greater ET in forests than in pastures (von Randow et al., 2004; Tanaka et al., 2008). The average daily ET values used during dry and

wet seasons for mature forests were 4.6 mm d^{-1} and 2.5 mm d^{-1}, respectively, based on upscaled sap flow measurements from the study catchments in Central Panama (Cheng et al., 2018). For pastures, the same ET value of 2.35 mm d^{-1} was used for both dry and wet seasons based on eddy flux tower measurements from study catchments in the PCW (Cheng et al., 2018). The ET for each of the seven study catchments during the dry and wet seasons was estimated using weights of mature forest and pasture derived from the land cover map (Figure 1; Table 1):

$$\begin{aligned} ET_{dry} &= ET_{dry}^{for} \times f_{for} + ET_{dry}^{pas} \times f_{pas}\text{, and} \\ ET_{wet} &= ET_{wet}^{for} \times f_{for} + ET_{wet}^{pas} \times f_{pas} \end{aligned} \quad (7)$$

where ET_{dry} and ET_{wet} are the estimated daily ET depths at each study catchment for dry and wet seasons, respectively (L); ET_{dry}^{for} and ET_{wet}^{for} are the daily ET values for mature forest land cover during the dry and wet seasons, respectively (L); ET_{dry}^{pas} and ET_{wet}^{pas} are the daily ET values for pasture land cover during the dry and wet seasons, respectively (L); and f_{for} and f_{pas} are the fractions (0~1) of forest and pasture land covers (Table 1), respectively, at each study catchment.

3.5 Sensitivity analysis

The correlations of the tested predictors can provide insights to the causes of BFJs. Regression model sensitivity analysis following Xu and Gertner (2008) and Pan et al. (2011) as shown in Equations 8 to 11 was used to assess the relative contribution of each predictor. These were evaluated in terms of their ability to predict the variances in the BFJs and quantify their independent contributions and joint contributions explained by their correlations with other predictors. The analysis can apportion the relative contributions of predictors in explaining the BFJ variance and rank their relative importance as predictors for the BFJ phenomena.

$$V = var(s) = \frac{1}{n-1}\sum_{i=1}^{n}(s_i - \bar{s})^2 \quad (8)$$

where V is total variance of the BFJ variable of either magnitude or timing, n is the number of data points, s is the BFJ magnitude (L T^{-1}) or timing (T), and $\bar{s}$ is the mean of the corresponding BFJ variable.

$$\hat{s}_i^j = a_0 + a_j x_{ij}, \qquad i = 1, 2, \ldots n \quad \text{and} \quad \hat{V}_j = \frac{1}{n-1}\sum_{i=1}^{n}\left(\hat{s}_i^j - \bar{s}\right)^2 \quad (9)$$

where $\hat{s}_i^j$ is the regression estimation of BFJ variable s_i by predictor x_j alone based on Equation 9, a_0 and a_j are the regression coefficients of predictor x_j, and $\hat{V}_j$ is the partial variance of BFJ variable contributed by predictor x_j.

$$\hat{s}_i^{-j} = b_0 + b_j \hat{z}_{ij}, i = 1, 2, \ldots n \quad \text{and} \quad \hat{V}_j^U = \frac{1}{n-1}\sum_{i=1}^{n}\left(\hat{s}_i^{-j} - \bar{s}\right)^2 \quad (10)$$

where $\hat{z}_{ij} = x_{ij} - \hat{x}_{ij}$ with $\hat{x}_{ij} = c_0 + \sum_{\substack{p=1 \\ p\neq j}}^{k} c_p x_{ip}$, $\hat{s}_i^{-j}$ is the regression estimation of BFJ variable s_i without predictor x_j by Equation 10, b_0, c_0, b_j and c_p are regression coefficients, and $\hat{V}_j^U$ is the partial variance contributed by the uncorrelated variance of predictor x_j.

$$S_j = \frac{\hat{V}_j}{V}, \qquad SU_j = \frac{\hat{V}_j^U}{V}, \qquad SC_j = \frac{\hat{V}_j^C}{V} = S_j - SU_j \quad (11)$$

where S_j, SU_j, and SC_j are total, uncorrelated, and correlated partial sensitivity indices of predictor x_j, respectively.

The total sensitivity index S_j, is a measurement of the total relative contribution to the variance of the BFJ variable from predictor x_j. The uncorrelated sensitivity index SU_j, is used to quantify the contribution that uniquely from x_j, and the correlated sensitivity index SC_j, is used to measure the contribution from x_j due to its correlation with other predictors.

3.6 Significant test

We applied the Student's t-test to test for significant differences between the results derived from the two base flow separation methods. We also tested for significant differences in timing and magnitude of the BFJs between the eastern and the western catchments. If the p value from the test is larger than the significant level p_0 (typically $p_0 = 0.05$), the null hypothesis that there is no significant difference between the two is accepted. When the null hypothesis is rejected (i.e., $p < p_0$), the detection of a significant difference is possible. Overall, a larger p-value is associated with stronger evidence of no significant difference.

4. Results

4.1 Catchment rainfall, runoff, and base flow

Based on the rainfall data available for the period from 1972 to 2012, annual rainfall for the study catchments in the western PCW varied between 1900 and 3150 mm y^{-1}, with a median value of 2460 mm y^{-1}. In the eastern PCW catchments, annual rainfall varied from 1950 to 4680 mm y^{-1}, with a median value of 3470 mm y^{-1}. This difference shows the significant orographic effect on annual rainfall caused by the approximately 1000 m tall mountains in the eastern PCW. It rained almost every day during the wet season. The average daily rainfall depth during the wet season at the western (eastern) PCW varied from 7.6 (7.8) to 12.7 (18.9) mm d^{-1}. The median values of daily rainfall were 9.9 and 13.4 mm d^{-1} for catchments in the western and eastern PCW, respectively. October and November were the months that on average had the highest rainfall totals.

The catchment average rainfall per event in the western PCW ranged from 3 to 290 mm, with

a median value of 16 mm. In the eastern PCW, the catchment average rainfall during events varied from 3 to 335 mm, with a median value of 15 mm. The average duration of rainfall events ranged from 0.1 to 19 hours at the western catchments and varied from 0.1 to 20 hours in the eastern catchments. The median durations for rainfall events were 2.5 and 3 hours for western and eastern PCW catchments, respectively.

During the same 41-year study period, the annual discharge from catchments in the western PCW varied between 550 and 2640 mm y^{-1}, with a median value of 1380 mm y^{-1}. The annual discharge at the eastern PCW catchments ranged from 780 to 4290 mm y^{-1}, with a median value of 2380 mm y^{-1}.

When it comes to base flow, the recession parameter (*a*) and the maximum value of the base flow index (BFI_{max}) calculated using the E2005 approach for each study catchment are listed in Table 2. The recession coefficient *a* varied between 0.94 to 0.97, and BFI_{max} ranged from 0.78 to 0.89. At catchments in the western PCW, the annual base flow as percent of rainfall varied from 31% to 63%, with a median value of 45%, while those catchments in the eastern PCW experienced greater annual base flow as percent of rainfall, ranging from 41% to 81%, with a median of 61%.

Table 2

4.2 BFJ timing and magnitude

Boxplots for both BFJ timing and magnitude based on the two base flow separation methods (E2005 and B2008) are shown in Figure 3. The median timing of the BFJ occurred on 218 and 226 days of the year (DOY) using the E2005 and B2008 methods, respectively, while median magnitudes of the jump were 2.7 and 2.2 mm d^{-1} using these two methods, respectively (Figure

3). Table 2 gives values of a and BFI_{max} for base flows before and after BFJs at the seven catchments, calculated using the E2005 approach. Base flow is more dominant in streamflow and recesses slower after the jump (Table 2).

Figure 3 also separates the jump results at catchments in the eastern and western PCW based on the same two separation methods. The 25th quantiles for jump magnitudes at western and eastern PCW catchments were 1.47 and 1.29 mm d $^{-1}$, respectively, and the 75th quantiles were 3.38 and 4.76 mm d $^{-1}$, respectively, using the E2005 base flow separation method (Figure 3b). When using the B2008 method, the 25th quantiles for jump magnitudes at western and eastern PCW were 1.28 and 1.24 mm d $^{-1}$, and the 75th quantiles were 3.08 and 3.64 mm d $^{-1}$, respectively (Figure 3b). The *p*-value according to the Student's t-test for jump timing at eastern and western PCW is 0.42, which means the timing of BFJ did not differ much across different locations. For jump magnitude at eastern and western PCW, the *p*-value according to the Student's t-test is 0.01, which means the difference in BJF magnitude between eastern and western PCW catchments is significant. The higher jump magnitudes in the eastern PCW catchments using both base flow separation methods indicate that these eastern catchments were more likely to generate larger BFJs.

Figure 3

Figure 4 shows scatterplots of BFJ timing and magnitude based on the two base flow separation methods. The BFJs were also separated into eastern and western PCW. The correlation between jump timing and magnitude in the eastern PCW catchments ($r_{\mathrm{E2005}}^{\mathrm{eastern}}$ = 0.6, $r_{\mathrm{B2008}}^{\mathrm{eastern}}$ = 0.41) was higher than that in the western PCW catchments ($r_{\mathrm{E2005}}^{\mathrm{western}}$ = 0.22, $r_{\mathrm{B2008}}^{\mathrm{western}}$ = 0.14) (Figures 4) when using both E2005 and B2008 methods. This higher correlation between

the jump timing and magnitude in the eastern PCW catchments is consistent with the previous finding that the eastern PCW catchments were more likely to produce larger jumps.

Figure 4

4.3 Sensitivity analysis and BFJ predictability

4.3.1 Watershed related predictors

The *p* values from the Student's t-test for the two base flow separation methods are 0.08 and 0.57 for jump timing and magnitude, respectively, which means both base flow separation methods produced similar BFJ detection results. Results presented in Figures 3 and 4 further support this conclusion. Therefore, we use the jump results from the E2005 for subsequent sensitivity analysis. Figure 5 shows base flow jump magnitude against the fraction of the catchment under forest land cover (f_{for}) and catchment mean slope. The small values of jump magnitude were associated with low f_{for}, while the larger values of BFJ magnitude occurred generally at greater f_{for} (Figure 5a). A similar trend was observed between jump magnitude and mean land surface slope (Figure 5b). Note the catchments with mean slope greater than 17° and with f_{for} greater than 26% are all in the eastern PCW. The higher likelihood that catchments in the eastern PCW always produce larger BFJs as discussed earlier was therefore attributable to their steeper land surface slopes and greater fraction of forest land covers. There is no clear trend, however, between BFJ timing and watershed physiography such as forest cover and mean slope. This result complements the previous finding that the BFJ timing did not differ much across different locations.

Figure 5

4.3.2 Combination of watershed and rainfall predictors

Figures 6a and 6c show scatterplots of both observed and predicted jump timing and magnitude and their correlations (*r*). Figures 6a and 6c also separately show the BFJs in catchments in the western and eastern portions of the PCW. Figures 6b and 6d show the total sensitivity index (*S*), correlated sensitivity index (*SC*) and uncorrelated sensitivity index (*SU*) of the examined predictors for jump timing and magnitude, respectively.

Overall, reasonable agreement was found between observed and predicted jump timing and magnitude when both watershed and rainfall predictors were included as seen in Figures 6a and 6c. The correlations between observed and predicted jump timing and magnitude are 0.92 and 0.65, respectively. More variation was explained by the predictors for jump timing compared to jump magnitude (R^2_{tim} = 0.85, R^2_{mag} = 0.42).

For jump timing, the best predictors as demonstrated by the total sensitivity index (*S*) values were cumulative rainfall and subsurface storage ($S^{\mathrm{tim}}_{\mathrm{P_{cum}}}$ = 0.67, $S^{\mathrm{tim}}_{\mathrm{S_{gw}}}$= 0.43) (Figure 6b), while the instantaneous effect of events just prior to the jump is small (Figures 6b). However, the correlated sensitivity index (*SC*) of subsurface storage in explaining the jump timing variance was relatively high ($SC^{\mathrm{tim}}_{\mathrm{S_{gw}}}$ = 0.425). For example, the subsurface storage was directly derived from rainfall in Equation 6 and was expected to be somewhat correlated with the cumulative rainfall (*r* = 0.26).

For jump magnitude, catchments in the eastern PCW in general exhibited larger BFJ magnitude (Figure 6c), which is consistent with the significant difference of jump magnitude between eastern and western PCW catchments according to results of Student's t-test reported earlier. The best predictors for jump magnitude were cumulative rainfall and forest fraction ($S^{\mathrm{mag}}_{\mathrm{P_{cum}}}$ = 0.35, $S^{\mathrm{mag}}_{\mathrm{f_{for}}}$= 0.1) (Figure 6d). These two predictors contributed to the higher possibility

of eastern PCW catchments in producing larger jumps. However, the *SC* for these two most important predictors for both timing and magnitude of BFJ ($SC^{\mathrm{mag}}_{\mathrm{P_{cum}}}$ = 0.14, $SC^{\mathrm{mag}}_{\mathrm{f_{for}}}$ = 0.08) is also large, suggesting large variances of BFJ were explained by cross-correlations between predictors.

Figure 6

5. Discussion

5.1 Effects of rainfall and catchment characteristics on BFJ timing and magnitude

The best predictors for BFJ timing were cumulative rainfall and subsurface storage. Therefore, the observed sudden and sustained base flow jumps are the result of cumulative effect of rainfall and changes in subsurface storages during the wet season rather than an instantaneous response to a few rainfall events just prior to the jump. The effect of subsurface storage on base flow generation has also been reported earlier (e.g., Niedzialek, 2007; Price 2011). Using a conceptual model, Niedzialek (2007) found that a sharp increase in subsurface storage might explain the step-wise increases observed in base flow in upper Rio Chagres, Panama.

The best predictors for jump magnitude were cumulative rainfall and forest fraction. The role of forest fraction in explaining jump magnitude may be attributed to the larger subsurface storage and groundwater recharge in forest land covers than pastures. Due to the potential of forested catchments to produce more base flows during the dry season compared to pastured catchments in the humid tropics (Bruijnzeel, 1989, 2004; Ogden et al., 2013; Krishnaswamy et al., 2012, 2013) and different responses of BFJs observed in catchments with different land covers in this study, quantifying the effect of forest land cover on BFJ timing and magnitude is crucial to examine the extent to which reforestation can restore the dry-season base flow in seasonal tropics (Zhang et al., 2019).

5.2 Effects of cross-correlations between predictors

The large value of correlated sensitivity index between cumulative rainfall and forest land cover, which are the two most important predictors, suggested that large variances were explained by their joint correlations, rather than their isolated contributions. This was also evident from the fact that the eastern PCW receives higher annual rainfall while also having a greater portion of forest cover. The results highlighted that the correlations between predictors, which few studies have addressed (Pan et al., 2011), should be considered to explain the jump timing and magnitude variances and predict the BFJ behaviors.

5.3 Broader applications and implications of this study

As a result of changes in hydrological processes under climate and environmental changes at a global scale (Montanari et al., 2013), changes in hydrological timeseries (e.g., streamflow, overland flow) have been observed not only in tropical regions, but also in many other regions around the world, in the form of either change-point (Salarijazi 2012; Xiong et al. 2015; Ivancic and Shaw, 2017) or trend (Pasquini and Depetris 2007; Schneider et al., 2013). This study proposed a framework to analyze sudden and sustained changes in base flow timeseries in the humid seasonal tropics, which can also be applied to other regions with similar seasonality as well as to examine sudden and sustained changes of other hydrological processes and variables (e.g., runoff generation, flooding).

Water supply in tropical regions is a critical ecosystem service but often inadequate due to human-induced changes and insufficient understanding of the hydrological processes in the humid tropics (Wohl et al., 2012). Water shortages are most severe in the 80% of the tropics with a pronounced dry season. Currently, the occurrence of very wet and very dry months was

amplified in response to anthropogenic warming over tropical regions (Lintner et al., 2012). Drought frequency and intensity is projected to increase under global warming in the 21st century (Cook et al., 2014). These changes intensify the pressures on water supply in tropical regions. The integrated statistical method proposed in this study is geared toward better quantitative characterization of the BFJ phenomenon (i.e., timing and magnitude, contributing factors). Since base flow is crucial to sustain water provisioning during the extended dry periods in tropics, this study has important ramifications for the effect of water and land management practices on the magnitude of dry-season low flows, especially under a changing environment.

5.4 Limitations and future work

Although this study identified some important factors affecting BFJ, base flow generation is a complicated process affected by a wide range of factors, such as watershed characteristics of geomorphology, soil, and land use, as well as the potential effects of global changes (Price 2011). Presently, subsurface storage observations are scant; if augmented, they could lead to improved prediction of BFJ timing and magnitude. Better understanding of water flow paths and the physical mechanisms behind the BFJ phenomenon can be expected with the aid of further modeling studies when more subsurface observations become available. Given the fact there have been very few studies on this BFJ phenomenon, this study calls for more scientific efforts to further understand the hydrological processes involved in the BFJ phenomenon, including better BFJ models and better field characterizations, to help inform and guide future water and land management.

6. Summary and Conclusions

This study was concerned with a unique observational phenomenon in the seasonal-tropical Panama Canal Watershed (PCW) -- the occurrence of sudden base flow jumps (BFJs) that occur during mid-wet season and persist throughout the remainder of the wet season. Understanding the effects of catchment characteristics and rainfall on the occurrence and magnitude of these BFJs has land management implications in the PCW, which is an important watershed for the global economy, and other seasonal tropics.

We developed an integrated approach to efficiently detect and quantitatively define BFJ timing and magnitude. The method was used in conjunction with the sensitivity analysis to rank the contributions of watershed and rainfall predictors due to their isolated and cross correlation effects. We used streamflow and rainfall data from seven sub-catchments of the PCW with different land covers, topography, and orographic influence to better understand the factors affecting the sudden and sustained BFJs. Two base flow separation techniques were used to evaluate the effect of base flow separation methods on the results. A piecewise linear regression on the cumulative average base flow was developed for BFJ detection. The change point between the two segments of the cumulative average base flow time series fitted by the piecewise linear regression identified the BFJ occurrence. Three watershed predictors and four rainfall-related predictors were tested to examine their abilities to predict the sudden and sustained BFJ behavior. The three watershed characteristics were the fraction of forest land cover, catchment area, and mean land surface slope. The rainfall-related predictors were cumulative rainfall, subsurface storage, and cumulative rainfall and maximum intensity of three rainfall events that immediately prior the BFJ.

Different base flow separation methods did not result in apparent differences in the detected BFJ timing and magnitude results. Catchments in the more mountainous and forested eastern

portion of the PCW produced larger jumps, while BFJ timing does not differ much across different locations. Correlations between observed BFJ and BFJ predicted by watershed and rainfall-related predictors were 0.92 and 0.65 for timing and magnitude, respectively. Cumulative rainfall and forest cover were the top two contributors to the likelihood of producing larger jumps in the eastern PCW catchments. The cross-correlations between predictors explained more than 50% of the BFJ variances.

The role of forest fraction in explaining jump magnitude is potentially associated with the larger subsurface storage and groundwater recharge in forest land covers than pastures. Quantifying the effect of forest land cover on BFJ in tropical forests is crucial to help quantify the extent to which reforestation can enhance dry-season base flow in tropical catchments with seasonality. The attribution of this unusual base flow behavior to rainfall and watershed characteristics in tropics with distinct dry and wet seasons provides insights to understand the important base flow hydrologic processes in tropical catchments and the role of seasonal transitions of base flow generation in tropics under different land uses and land covers. Future modeling study when more subsurface observations become available will potentially provide insights to understand the water flow paths and better explain the physical hydrological processes behind this BFJ phenomenon. The improved understanding can better inform land management decisions for ecosystem services under a changing environment.

Data Availability Statement:

The land cover map was produced by the Panama Canal Authority and obtained from the Smithsonian Tropical Research Institute website (http://strimaps.si.edu/portal/home/item.html?id=eff3f5db4da94453bbab21dc1b557ee6).

Catchment areas, gauge locations and the rainfall and streamflow data at 15-minute interval for the seven examined catchments were produced by the Panama Canal Authority and retrieved from the Smithsonian Tropical Research Institute website (http://biogeodb.stri.si.edu/physical_monitoring/research/panamacanalauthority#download).

References

Adamowicz, W., Calderon-Etter, L., Entem, A., Fenichel, E. P., Hall, J. S., Lloyd-Smith, P., … Stallard, R. F. (2019). Assessing ecological infrastructure investments. *Proceedings of the National Academy of Sciences*, 116(12), 5254–5261. https://doi.org/10.1073/pnas.1802883116

Aksoy, H., Kurt, I., & Eris, E. (2009). Filtered smoothed minima baseflow separation method. *Journal of Hydrology*, 372(1–4), 94–101. https://doi.org/10.1016/j.jhydrol.2009.03.037

Arnold, J. G., & Allen, P. M. (1999). Automated methods for estimating baseflow and groundwater recharge from streamflow records. *Journal of the American Water Resources Association*, 35(2), 411–424. https://doi.org/10.1111/j.1752-1688.1999.tb03599.x

Beck, H. E., Van Dijk, A. I. J. M., Miralles, D. G., De Jeu, R. A. M., Bruijnzeel, L. A., McVicar, T. R., & Schellekens, J. (2013). Global patterns in base flow index and recession based on streamflow observations from 3394 catchments. *Water Resources Research*, 49(12), 7843–7863. https://doi.org/10.1002/2013WR013918

Bonell, M., & Bruijnzeel, L. A. (Eds.). (2005). *Forests, water and people in the humid tropics: past, present and future hydrological research for integrated land and water management*. Cambridge University Press, Cambridge, U.K.

575 Bretfeld, M., Ewers, B. E., & Hall, J. S. (2018). Plant water use responses along secondary forest
576 succession during the 2015–2016 El Niño drought in Panama. New Phytologist.
577 https://doi.org/10.1111/nph.15071
578 Bruijnzeel, L. A. (1989). (De-)Forestation and dry season flow in the tropics: A closer look.
579 *Journal of Tropical Forest Science*, 229-243.
580 Bruijnzeel, L. A. (2004). Hydrological functions of tropical forests: Not seeing the soil for the
581 trees? *Agriculture, Ecosystems and Environment* 104(1), 185-228.
582 https://doi.org/10.1016/j.agee.2004.01.015
583 Brutsaert, W. (2008). Long-term groundwater storage trends estimated from streamflow records:
584 Climatic perspective. *Water Resources Research*, 44(2), 1–7.
585 https://doi.org/10.1029/2007WR006518
586 Cadol, D., Kampf, S., & Wohl, E. (2012). Effects of evapotranspiration on baseflow in a tropical
587 headwater catchment. *Journal of Hydrology*, 462–463, 4–14.
588 https://doi.org/10.1016/j.jhydrol.2012.04.060
589 Callaghan, J., & Bonell M. (2005), An overview of the meteorology and climatology of the
590 humid tropics, in *Forests, Water and People in the Humid Tropics: Past, Present and Future*
591 *Hydrological Research for Integrated Land and Water Management*, edited by M. Bonell
592 and L. Bruijnzeel, pp. 158–193, UNESCO, Cambridge Univ. Press, Cambridge.
593 Chapman, T. (1999). A comparison of algorithms for streamflow recession and baseflow
594 separation. *Hydrological Processes*, 13(July 1998), 701–714.
595 https://doi.org/10.1002/(SICI)1099-1085(19990415)13:5<701::AID-HYP774>3.0.CO;2-2

596 Chapman, T. G., & Maxwell, A. I. (1996). Baseflow separation-comparison of numerical
597 methods with tracer experiments. *In Hydrology and Water Resources Symposium 1996:*
598 *Water and the Environment; Preprints of Papers (p. 539)*. Institution of Engineers, Australia.
599 Cheng, Y., Ogden, F. L., & Zhu, J. (2017). Earthworms and tree roots: A model study of the
600 effect of preferential flow paths on runoff generation and groundwater recharge in steep,
601 saprolitic, tropical lowland catchments. *Water Resources Research*, 53.
602 https://doi.org/10.1002/2016WR020258
603 Cheng, Y., Ogden, F. L., Zhu, J., & Bretfeld, M. (2018). Land use dependent preferential flow
604 paths affect hydrological response of steep tropical lowland catchments with saprolitic soils.
605 *Water Resources Research*. https://doi.org/10.1029/2017WR021875
606 Chow, V. T., Maidment, D. R. & Larry, W., Mays, (1988). Applied Hydrology. McGraw- Hill:
607 Singapore; 572.
608 Collischonn, W., & Fan, F. M. (2013). Defining parameters for Eckhardt's digital baseflow filter.
609 *Hydrological Processes*, 27(18), 2614–2622. https://doi.org/10.1002/hyp.9391
610 Cook, B. I., Smerdon, J. E., Seager, R., & Coats, S. (2014). Global warming and 21 st century
611 drying. Climate Dynamics, 43(9–10), 2607–2627. https://doi.org/10.1007/s00382-014-2075-
612 y
613 Eckhardt, K. (2005). How to construct recursive digital filters for baseflow separation.
614 *Hydrological Processes*, 19(2), 507–515. https://doi.org/10.1002/hyp.5675
615 Harmon, R. S. (2005a). An introduction to the Panama Canal watershed, in *The Rio Chagres,*
616 *Panama: A Multidisciplinary Profile of a Tropical Watershed*, edited by R. S. Harmon, pp.
617 19–29, Springer, Dordrecht, Netherlands.

Harmon, R. S. (2005b). The geological development of Panama, in The Rio Chagres, Panama: A Multidisciplinary Profile of a Tropical Watershed, edited by R. S. Harmon, pp. 45–64, Springer, Dordrecht, Netherlands.

Harmon, R. S., Lyons, W. B., Long, D. T., Ogden, F. L., Mitasova, H., Gardner, C. B., ... & Witherow, R. A. (2009). Geochemistry of four tropical montane watersheds, Central Panama. *Applied Geochemistry*, 24(4), 624-640.

Knight, K. (2008). The implications of Panama Canal expansion to US ports and coastal navigation economic analysis. Institute for Water Resources, US Army Corps of Engineers, 27.

Krishnaswamy, J., Bonell, M., Venkatesh, B., Purandara, B. K., Rakesh, K. N., Lele, S., … Badiger, S. (2013). The groundwater recharge response and hydrologic services of tropical humid forest ecosystems to use and reforestation: Support for the "infiltration-evapotranspiration trade-off hypothesis." *Journal of Hydrology*, 498, 191–209. https://doi.org/10.1016/j.jhydrol.2013.06.034

Krishnaswamy, J., Bonell, M., Venkatesh, B., Purandara, B. K., Lele, S., Kiran, M. C., et al. (2012). The rain-runoff response of tropical humid forest ecosystems to use and reforestation in the Western Ghats of India. Journal of Hydrology, 472–473, 216–237. https://doi.org/10.1016/j.jhydrol.2012.09.016

Ladouche, B., Probst, A., Viville, D., Idir, S., Baqué, D., Loubet, M., … Bariac, T. (2001). Hydrograph separation using isotopic, chemical and hydrological approaches (Strengbach catchment, France). *Journal of Hydrology*, 242(3–4), 255–274. https://doi.org/10.1016/S0022-1694(00)00391-7

Lintner, B. R., Biasutti, M., Diffenbaugh, N. S., Lee, J. E., Niznik, M. J., & Findell, K. L. (2012). Amplification of wet and dry month occurrence over tropical land regions in response to global warming. *Journal of Geophysical Research Atmospheres*, 117(11), 1–10. https://doi.org/10.1029/2012JD017499

Lyne, V., & Hollick, M. (1979, September). Stochastic time-variable rainfall-runoff modelling. In Institute of Engineers Australia National Conference (Vol. 1979, pp. 89-93).

Ivancic, T. J., & Shaw, S. B. (2017). Identifying spatial clustering in change points of streamflow across the contiguous U.S. between 1945 and 2009. *Geophysical Research Letters*, 2445–2453. https://doi.org/10.1002/2016GL072444

Montanari, A., Young, G., Savenije, H. H. G., Hughes, D., Wagener, T., Ren, L. L., … Belyaev, V. (2013). "Panta Rhei-Everything Flows": Change in hydrology and society-The IAHS Scientific Decade 2013-2022. Hydrological Sciences Journal, 58(6), 1256–1275. https://doi.org/10.1080/02626667.2013.809088

Montgomery Watson Harza (MWH) (2001). Study of Variations and Trends in the Historical Rainfall and Runoff Data in the Gatun Lake Watershed, Volume 1—Main Report, 262 pp., Autoridad del Canal de Panama, Balboa, Republic of Panama.

Muñoz-Villers, L. E., Geissert, D. R., Holwerda, F., & McDonnell, J. J. (2016). Factors influencing stream baseflow transit times in tropical montane watersheds. *Hydrology and Earth System Sciences*, 20(4), 1621–1635. https://doi.org/10.5194/hess-20-1621-2016

Nathan, R. J., & McMahon, T. A. (1990). Evaluation of automated techniques for base flow and recession analyses. *Water Resources Research*, 26(7), 1465–1473. https://doi.org/10.1029/WR026i007p01465

Niedzialek, J., 2007. Unusual hydrograph characteristics, Upper Rio Chagres, PhD dissertation,

Dept. of Civil and Environmental Engineering, Univ. of Connecticut, Storrs, Conn.

Niedzialek, J. M. & Ogden F. L. (2005). Runoff production in the upper Río Chagres watershed, Panama. In *The Río Chagres, Panama* (pp. 149-168). Springer Netherlands.

Niedzialek, J. M., & Ogden, F. L. (2012). First-order catchment mass balance during the wet season in the Panama Canal Watershed. *Journal of Hydrology*, 462–463, 77–86. https://doi.org/10.1016/j.jhydrol.2010.07.044

Ogden, F. L., Crouch, T. D., Stallard, R. F., & Hall, J. S. (2013). Effect of land cover and use on dry season river runoff, runoff efficiency, and peak storm runoff in the seasonal tropics of Central Panama. *Water Resources Research*, 49(12), 8443–8462. https://doi.org/10.1002/2013WR013956

Ogden, F. L., Mojica A., and Abebe N. A. (2010). Ecohydrologic investigations of shallow lateral subsurface flow in tropical soils using time-lapse surface electrical resistivity tomography, Abstract H51J-07 presented at 2010 Fall Meeting, AGU, San Francisco, Calif.

Pan, F., Zhu, J., Ye, M., Pachepsky, Y. A., & Wu, Y. S. (2011). Sensitivity analysis of unsaturated flow and contaminant transport with correlated parameters. *Journal of Hydrology*, 397(3–4), 238–249. https://doi.org/10.1016/j.jhydrol.2010.11.045

Pasquini, A. I., & Depetris, P. J. (2007). Discharge trends and flow dynamics of South American rivers draining the southern Atlantic seaboard: An overview. *Journal of Hydrology*, 333(2–4), 385–399. https://doi.org/10.1016/j.jhydrol.2006.09.005

Pena-Arancibia, J. L., Van Dijk, A. I. J. M., Mulligan, M., & Bruijnzeel, L. A. (2010). The role of climatic and terrain attributes in estimating baseflow recession in tropical catchments. *Hydrology and Earth System Sciences*, 14(11), 2193–2205. https://doi.org/10.5194/hess-14-2193-2010

686 Price, K. (2011). Effects of watershed topography, soils, land use, and climate on baseflow
687 hydrology in humid regions: A review. *Progress in Physical Geography*, 35(4), 465–492.
688 https://doi.org/10.1177/0309133311402714
689 Salarijazi, M. (2012). Trend and change-point detection for the annual stream-flow series of the
690 Karun River at the Ahvaz hydrometric station. *African Journal of Agricultural Research*,
691 7(32), 4540–4552. https://doi.org/10.5897/ajar12.650
692 Schneider, C., Laizé, C. L. R., Acreman, M. C., & Flörke, M. (2013). How will climate change
693 modify river flow regimes in Europe? *Hydrology and Earth System Sciences*, 17(1), 325–339.
694 https://doi.org/10.5194/hess-17-325-2013
695 Stewart, R. H., & Stewart, J. L. (1980). Geologic map of the Panama Canal and vicinity,
696 Republic of Panama (No. 1232).
697 Tanaka, N., Kume, T., Yoshifuji, N., Tanaka, K., Takizawa, H., Shiraki, K., Tantasirin, C.,
698 Tangtham, N., & Suzuki, M. (2008). A review of evapotranspiration estimates from tropical
699 forests in Thailand and adjacent regions. *Agricultural and Forest Meteorology*, 148(5), 807-
700 819. https://doi.org/10.1016/j.agrformet.2008.01.011
701 Turner, B. L., & Engelbrecht, B. M. (2011). Soil organic phosphorus in lowland tropical rain
702 forests. *Biogeochemistry*, 103(1-3), 297-315.
703 van Dijk, a. I. J. M. (2010). Climate and terrain factors explaining streamflow response and
704 recession in Australian catchments. *Hydrology and Earth System Sciences*, 14(1), 159–169.
705 https://doi.org/10.5194/hess-14-159-2010
706 von Randow, C., Manzi, A. O., Kruijt, B., de Oliveira, P. J., Zanchi, F. B., Silva, R. L., Hodnett,
707 M. G., Gash, J. H. C., Elbers, J. A., Waterloo, M. J., Cardoso, F. L., & Kabat, P. (2004).
708 Comparative measurements and seasonal variations in energy and carbon exchange over

709 forest and pasture in South West Amazonia. *Theoretical and Applied Climatology*, 78(1–3),
710 5–26. https://doi.org/10.1007/s00704-004-0041-z
711 Wohl, E., Barros, A., Brunsell, N., Chappell, N. A., Coe, M., Giambelluca, T., … Ogden, F.
712 (2012). The hydrology of the humid tropics. *Nature Climate Change*, 2(9), 655–662.
713 https://doi.org/10.1038/nclimate1556
714 Wörner, G., Harmon, R., Hartmann, G., & Simon, K. (2005). Igneous geology and geochemistry
715 of the Upper Río Chagres Basin. *The Río Chagres, Panama*, 65-81.
716 Xiong, L., Jiang, C., Xu, C. Y., Yu, K. X., & Guo, S. (2015). A framework of change-point
717 detection for multivariate hydrological series. *Water Resources Research*, 51(10), 8198–8217.
718 https://doi.org/10.1002/2015WR017677
719 Xu, C., & Gertner, G. Z. (2008). Uncertainty and sensitivity analysis for models with correlated
720 parameters. *Reliability Engineering and System Safety*, 93(10), 1563–1573.
721 https://doi.org/10.1016/j.ress.2007.06.003
722 Zhang J. 2018. Hydrological response of a fire- climax grassland and a reforest before and after
723 passage of Typhoon Haiyan (Leyte Island, the Philippines). Thesis (PhD), VU University,
724 Amsterdam, The Netherlands, 268 pp.
725 Zhang, J., Bruijnzeel, L. A., Quiñones, M. C., Tripoli, R., Asio, V. B., & van Meerveld, H. J.
726 (2019). Soil physical characteristics of a degraded tropical grassland and a 'reforest':
727 Implications for runoff generation. Geoderma, 333, 163–177,
728 https://doi.org/10.1016/j.geoderma.2018.07.022.

LIST OF TABLES:

Table 1: Characteristics of the seven study catchments in this study

Table 2: Base flow separation parameter values for the seven study catchments for the entire streamflow time series, before BFJ, and after BFJ, using the approach of Eckhardt (2005).

LIST OF FIGURES:

Figure 1: (a) Location of Panama and (b) locations and land cover types of the seven study catchments in the Panama Canal Watershed.

Figure 2: Schematic of the BFJ detection method using the wet season data from 1 May 2012 to 31 December 2012 at the Gatun catchment as an example: (a) original data (streamflow and base flow), and (b) cumulative average of base flow. The linear lines in (b) are fitted curves using piecewise linear regression to detect the change date.

Figure 3: Box plot for BFJ (a) timing and (b) magnitude based on two base flow separation methods (E2005 and B2008) with median values in the parentheses. Western and eastern indicate that jump occurred at catchments in the western and eastern Panama Canal Watershed, respectively. The central bar is the median, the upper and lower limits of the box represent the 25^{th} and 75^{th} quantiles, while the whiskers represent the 5^{th} and 95^{th} percentiles. Symbols denote maximum and minimum values.

Figure 4: Scatter plots of BFJ timing and magnitude based on two base flow separation methods: (a) E2005, (b) B2008. Western and eastern in (a) and (b) indicate that jump occurred at catchments in the western and eastern Panama Canal Watershed, respectively.

Figure 5: Box plot for BFJ magnitude at the seven study catchments arranged by: (a) the fraction of the catchment under forest land cover f_{for}, and (b) catchment mean slope. The number in

752 parentheses in the upper row is the median, and the number in parentheses in the lower row is
753 the mean values. The central bar is the median, the upper and lower limits of the box
754 represent the 25^{th} and 75^{th} quantiles, while the whiskers represent the 5^{th} and 95^{th} percentiles.
755 Symbols denote maximum and minimum values.

756 **Figure 6:** Scatter plots of observed and predicted (a) BFJ timing, (c) BFJ magnitude estimated
757 from both rainfall and watershed attributes and sensitivity indices (total sensitivity index *S*,
758 correlated sensitivity index *SC* and uncorrelated sensitivity index *SU*) of each predictor for (b)
759 jump timing, (d) jump magnitude. Western and eastern indicate that jump occurred at
760 catchments in the western and eastern Panama Canal Watershed, respectively.

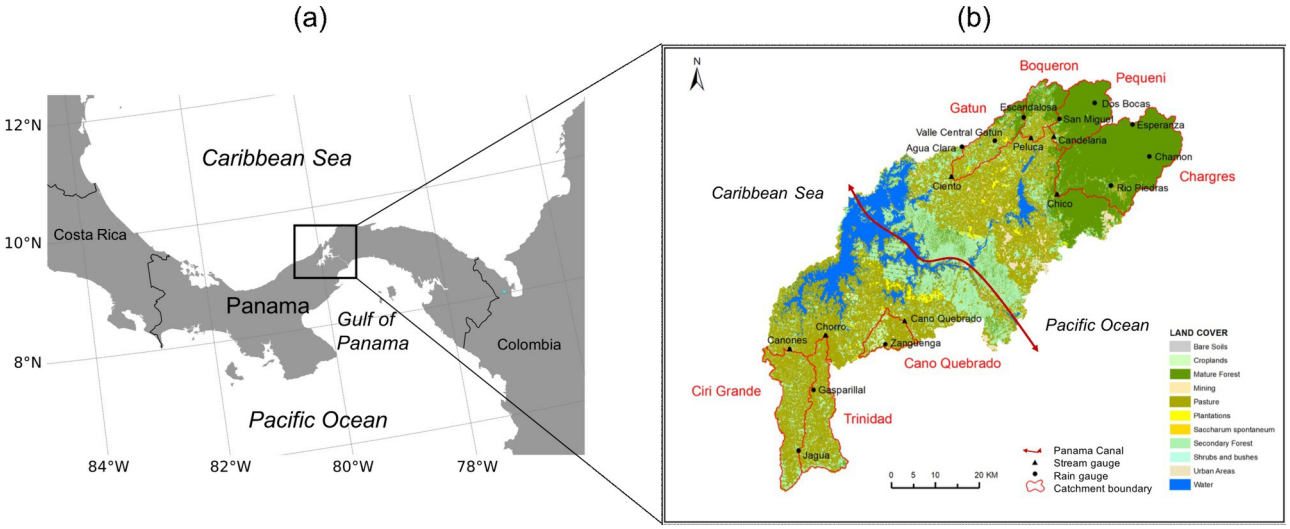

hyp_13604_figure1.eps

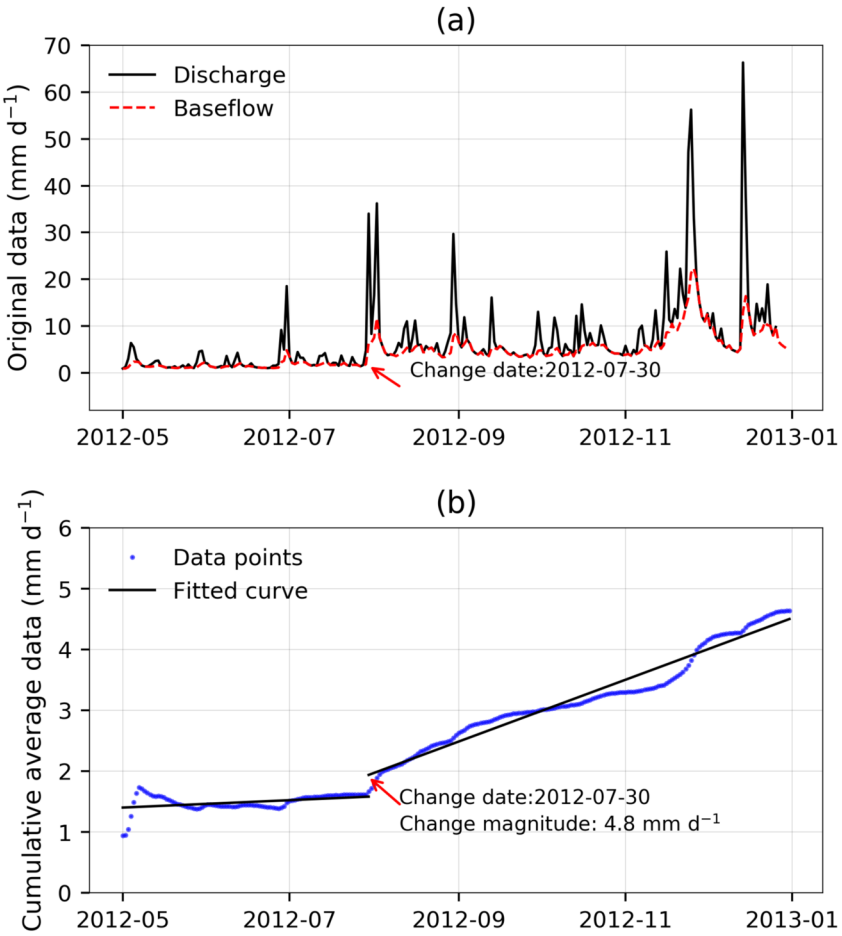

HYP_13604_Figure2.tif

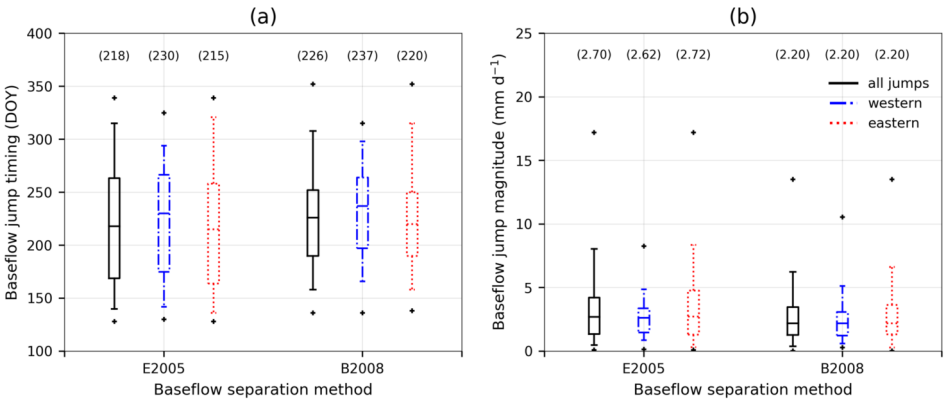

HYP_13604_Figure3l.tif

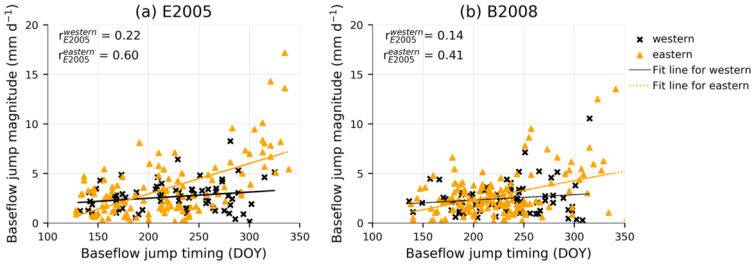

HYP_13604_Figure4.tif

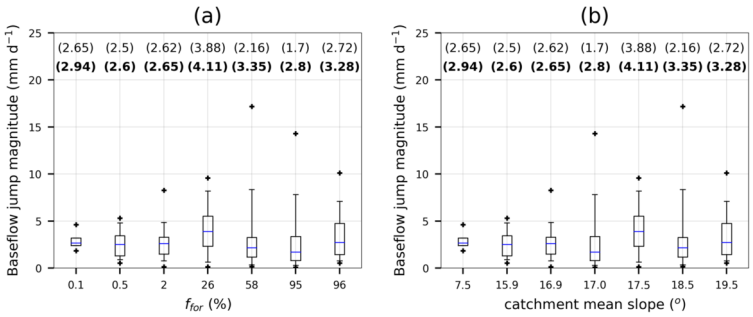

HYP_13604_Figure5.tif

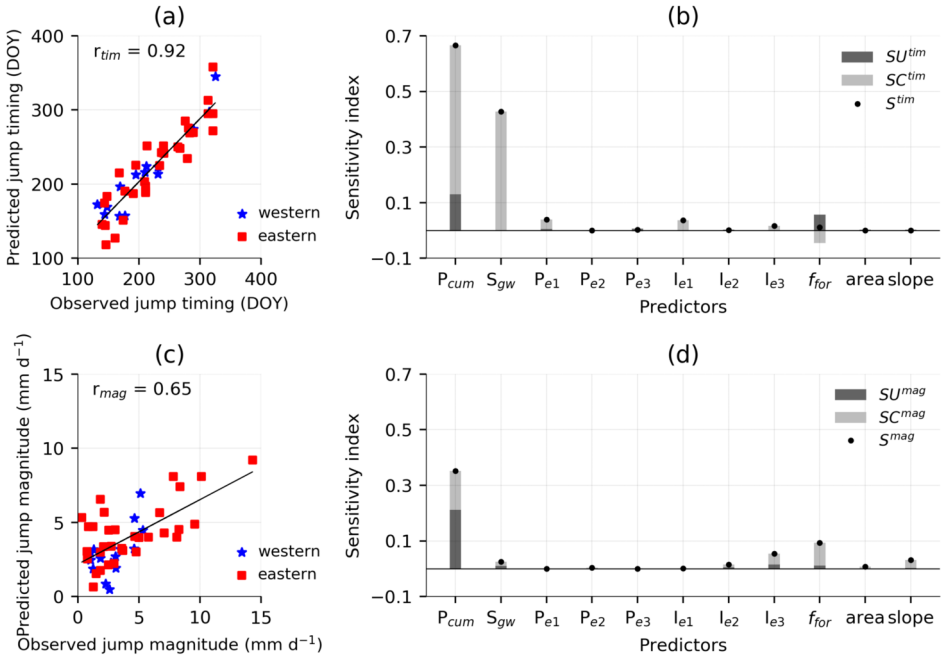

HYP_13604_Figure6.tif